CrystEngComm

Accepted Manuscript

ROYAL SOCIETY OF CHEMISTRY

www.rsc.org/crystengcomm

Cite this: DOI: 10.1039/c0xx00000x

www.rsc.org/xxxxxx

ARTICLE TYPE

Tunable Growth of PbS Quantum Dots-ZnO Heterostructure and Mechanism Analysis

Haili Li,[a] Shujie Jiao, *[a, b] Hongtao Li,[a] Lin Li[b] and Xitian Zhang[b]

Received (in XXX, XXX) Xth XXXXXXXXX 20XX, Accepted Xth XXXXXXXXX 20XX

DOI: 10.1039/b000000x

Potential applications of quantum dots–on-wide bandgap semiconductor structure in flexible and large-scale optoelectronics demand fundamental analysis on their tunable growth. Herein, PbS quantum dots (<5 nm)-on-ZnO heterostructure is formed by successive ionic layer adsorption and reaction method. Well distributed PbS quantum dots on ZnO is achieved just by changing solvent of $Pb(NO_3)_2$ and analyzed from the view of solvent-related interaction and adhesion between hydrophobic substrate and self-assembles layers. This solvent-related distribution of PbS quantum dots on ZnO is confirmed by scanning electron microscope and transmission electron microscope, which shows that fine distribution of PbS quantum dots on ZnO is feasible by using more ethanol in the solvent of $Pb(NO_3)_2$. With the aim towards tunable growth of PbS-on-ZnO heterostructure, effects of concentration and dipping times on the size and structure of PbS quantum dots are also explored, which demonstrates that the size of quantum dots is mainly thermodynamic domains. Meanwhile, the stoichiometric ratio of Pb and S can also be tuned by changing dipping times. Most significantly, their optical and electrical properties also show an obvious solvent-related characteristic, which provides another key factor for the potential fabrication and application of quantum dots based devices.

Introduction

It is commonly believed that growth control at nanoscale plays a key role for applications of desirable devices with high performance, reduced size and "soft" characteristics. Fine control on materials growth at nanoscale facilitate technical applicaitons by rendering materials with exactly suitable structures and characteristics. With the rapid development in optoelectronics, quantum dots (QDs)-on-wide bandgap semiconductor structure have attract increasing interests and great achievements have been achieved recently.[1-5] Even though many investigations have been carried out for PbS QDs, such as the discovery of size related band gap modulation and multiple exciton generation (MEG) process dominated carrier multiplications in PbS QDs solar cells which may even promote the ultimate theoretical Shockley-Queisser limit for photon-to-electron energy conversion (30%). However, effective fabrication of PbS-based heterostructure is still a puzzle.[6,7] Many methods have thus been introduced for fabrications of various QDs-based structures.[8-12] Among them, the low cost successive ionic layer adsorption and reaction (SILAR) method, which can be performed at mild conditions with unnecessary expensive apparatus, attracts the most attention.[13-14] Many QDs have been fabricated by SILAR method, it is still a challenge for effective fabrication of QDs-based heterostructures by this method due to the manifold effects of fabrication techniques on the final products.[15-17] Two major confronting issues are mentioned: (I) Aggregation of PbS QDs; (II) Effectively control on the size and stoichiometric ratio of Pb and S. Indeed, the quantum effect of QDs are closely size dependent[4] and variations in the stoichiometric ratio of Pb/S have the potential for bandgap modulation of PbS QDs.[18] What's more, the depletion width in semiconductor, which is the key parameter for heterostructure applications, can also be tuned by stoichiometric ratio of Pb/S in PbS QDs based on the fact that the surface traps states of PbS QDs including non-stoichiometric surface compositions and incomplete passivation.[19] Thus, systematic analysis on the growth mechanism of PbS QDs on ZnO is of great significance to their application directed materials growth and eventually realization of miniaturized QDs-on-Semiconductor based devices with excellent performance.

Herein, PbS QDs on ZnO heterostructure is formed by SILAR method and the distribution of PbS QDs on ZnO is explored from the view of adhesion architecture of growth cells at the solid-liquid interfaces based on the fact that SILAR method belongs to surface approach in which the surface contact reaches comparable dimensions. The size control of QDs is mainly achieved from the aspect of thermodynamic. The effects of materials formation on the stoichiometric ratios of Pb and S in PbS QDs as well as the optical and electrical properties of the as-synthesized PbS QDs-on-ZnO heterostructures are also explored.

Experimental Section

Preparation of different ZnO nanostructures

ZnO nanomaterials mentioned here including ZnO

nanocolumns (NCs) and ZnO nanowires (NWs) were formed by hydrothermal method at low temperature as mentioned before.[20] ZnO seed layers were firstly formed on the ITO substrate by sol-gel based dip coating method as mentioned in our previous work, but with some modifications.[21] The substrate was dried at 150 ^{o}C for 30 min after being pulled out at the rate of 5 cm/min and the seed layer were formed by repeating the above procedures for two times and finally annealed at 300 ^{o}C for 30 min. Different ZnO nanostructures were formed by hydrothermal method at 90 ^{o}C for 4 h with the conductive side down, but in different aqueous solutions: For ZnO NWs, the nutrient solution is consisted of $Zn(AC)_2{\cdot}2H_2O$ (0.03 M) and HMT (0.03 M); For ZnO NCs, only $Zn(AC)_2{\cdot}2H_2O$ (0.12 M) is involved. After reaction, reactors were cooled in cold water bath (22 ^{o}C) immediately for 1 min. Eventually, the sample was picked out and dried at room temperature after being rinsed with deionized water thoroughly.

Formation of PbS quantum dots on ZnO by SILAR method

Typical procedures for the formation of PbS QDs on ZnO are as follows: (I) The substrate was firstly immersed into $Pb(NO_3)_2$ solutions for 30 s; (II) Washed by pure ethanol and blew to dry; (III) The substrate was then immersed into Na_2S solutions for 1 min; (IV) Washed by pure ethanol again and blew to dry. The samples (S1-S5) were formed by repeating these immersion cycles for some times. In this research, mixture with ethanol/water (1:1/v:v) was used as solvent of Na_2S solution and its concentration (0.05 M) is kept constant. While the solvents of $Pb(NO_3)_2$ solution for samples S1-S3 varied from pure ethanol and pure water to the mixture of ethanol and water while maintaining the concentration of $Pb(NO_3)_2$ solution 0.02 M. Samples formed in $Pb(NO_3)_2$ solutions with ethanol/water volume ratios 1:1, 1:2 and 2:1 are marked as S1, S2 and S3. Effect of concentrations on the formation of PbS QDs was explored by changing the concentrations of $(Pb(NO_3)_2$ in the mixture of ethanol and water (2:1/v:v) from 0.02 M to 0.03 M (S4) and 0.04 M (S5). As for the effect of SILAR times on the formation of PbS QDs, one circle of SILAR process was defined as followings: SILAR procedures (I) and (II) mentioned above were firstly repeated for some times (3 times for S6 and 5 times for S7) followed by doing the procedures (III) and (IV) for one time. The samples S6 and S7 were formed by repeating this cycle for 5 times.

Characterization

Scanning electron microscope (SEM, KYKY-EM6000C, 15 KV) and Transmission electron microscope (TEM, Hitachi, H-7650) were used for structure and crystalline analysis of PbS QDs-ZnO heterostructures. Energy Dispersive Spectrum (EDS) were achieved by Bruker's Energy Disperse Spectroscopy (15 kV, HORIBA Jobin Yvon). Their optical properties and electrical properties were performed by Ultraviolet-visible Spectra (UV 1700-1800, Fenghuang, Shanghai) and electrochemical workstation (Corrtest, CS350) with a three electrodes system.

Results and Discussion

Effects of growth parameters on PbS QDs

a. Effect of solvents

Generally, SILAR method is ascribed to be one of the chemical bath deposition methods, thus, the effect of solvent of $Pb(NO_3)_2$ on the formation of PbS QDs-on-ZnO heterostructure is firstly explored. Figure 1a is the SEM image of the as-synthesized ZnO NCs by hydrothermal method. Figures 1b-1c are SEM images of PbS QDs-on-ZnO heterostructures formed by SILAR method. Both samples were formed with the same procedures, but with pure ethanol and water as solvent of $Pb(NO_3)_2$ solutions, respectively. For the case when ethanol is used as solvent of $Pb(NO_3)_2$, the formation of QDs on ZnO NCs was a little hard to distinguish as shown in Figure 1b. Thus, EDS element mapping is necessary and its corresponding element distribution images are given in Figure 2.[22] The formation of PbS is confirmed by the uniformly distributed Pb and S elements besides Zn and O element. While on the condition when water was used as solvent of $Pb(NO_3)_2$ solution, larger size QDs clusters were formed randomly over the surface of ZnO NCs, as marked by green circle in Figure 1c. EDS characterization on both the cluster and its surroundings are performed as given in supporting information S1. Pb and S elements are observed in both sections, but the cluster contains more Pb and S elements. Besides, the colour of the sample also changes from white to dark brown and light brown with the formation of PbS on ZnO as shown in the inset images in Figure 1. This variation provides a macro evidence for the formation of PbS.[23]

Based on the above analysis, it is rational to deduce that agglomerations of PbS QDs are solvent-related and may be weakened by adding ethanol into the commonly used water solvent of $Pb(NO_3)_2$ solution. To confirm this deduction, SEM and TEM images of PbS QDs-ZnO heterostructures formed by using the mixture of ethanol and water with volume ratio 1:1 (S1) and 1:2 (S2) as solvents are given in Figure 3a-3c and Figure 3d-3f. As shown in their SEM images, the surfaces of ZnO NCs in Figure 3a and 3d became rougher owing to the formation

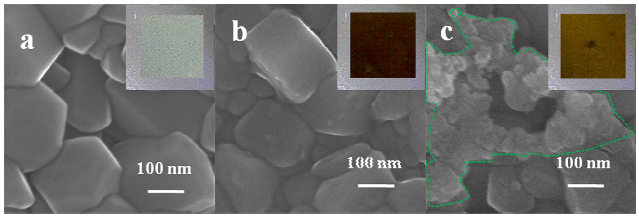

Figure 1 SEM images of (a) ZnO NCs; (b) and (c) PbS QDs-ZnO heterostructures formed by using pure ethanol and pure water as solvent of $Pb(NO_3)_2$. The insets shows the optical photographs of the corresponding samples.

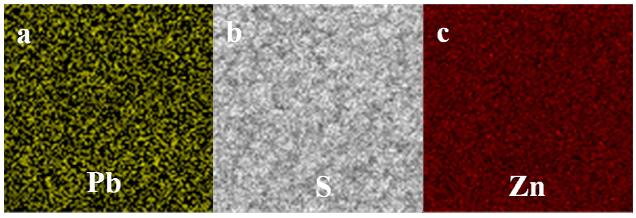

Figure 2 EDS element mapping images of PbS QDs-ZnO heterostructure formed by using pure ethanol as solvent of $Pb(NO_3)_2$.

of QDs on ZnO. The diffraction rings in Figure 2b and 2e are taken from the interface between PbS QDs and ZnO NCs of samples S1 and S2. The characterization results are in good accordance with the results in previous reports.[24-26] The diffraction rings marked by green and red circles in this report belong to ZnO and PbS, respectively. According to the analysis of diffraction ring, the sum of the squares of interference index of crystal plane (N) should be proportional to the square of radius of the corresponding diffraction ring. Calculation result confirms the existence of cubic PbS on ZnO. To present the structure and distribution of PbS QDs on ZnO more clearly, high magnitude TEM images are given in Figure 2c and 2f. It is obvious that PbS QDs formed by $Pb(NO_3)_2$ solution with ethanol/water volume ratio 1:2 (S1) are well distributed on the surface of ZnO. In contrast, with the proportion of water increased, PbS QDs clusters are observed beyond the surface of ZnO NC as marked by the red circle in Figure 2f.

In order to further confirm the effect of solvent on the formation of PbS QDs by SILAR method, the volume ratio of ethanol and water in the mixture solution of $Pb(NO_3)_2$ is further increased to 2:1 (S3). SEM and TEM results are shown in Figure 4. Similar to the samples formed in Figure 3, rough ZnO NCs (Figure 4a) and multiple diffraction rings (Figure 4b) belong to ZnO and PbS are observed. High magnitude TEM images in Figure 4c provides a thicker and successive distribution of PbS QDs on the surface of ZnO NCs. High resolution TEM of the as-synthesized QDs is given in Figure 4d, which shows elliptical QD structure. The lattice spacing is measured to be 0.34 nm corresponding to the (111) plane of cubic PbS.[22,27] More information on the high resolution TEM images of the as-synthesized sample is given in the supporting information S2.

Based on the above analysis, it is obvious that the distribution geometry of PbS QDs on ZnO is closely related with the solvent properties. This solvent-related formation of PbS QDs on hydrophobic ZnO can be explained by Charles F. Zukoski's adhesion model concerning on the dependence of contact angle of solution cluster on the surface of hydrophobic substrate.[28] In his theory, he pointed out that interactions near surfaces can be altered by changing the wetting properties of the surface and the depletion of fluid near such surfaces and eventually determines the distribution of PbS QDs on ZnO. It has been calculated by Thomas R. Weikl's by using hypernetted-chain approximation that the adhesive forces of mixtures of water and ethanol decrease with solvent dielectric constant and vary monotonically with their volume ratio.[29] According to his report, a smooth monotonic attraction would be found when the solvent-surface attraction is weak and significant depletion of fluid densities near such surfaces is then formed. Thus, the effect of solvent on the formation of PbS QDs can be totally understood based on the fact that increases in volume fraction of ethanol lead to decrease in the interaction of Pb^{2+} ions layer on the interfaces of ZnO.[28] Consequently, a uniform Pb^{2+} ions layer is dispersed on ZnO and eventually well-distributed PbS QDs.

b. Effect of concentration

The effect of concentration on the structure of PbS QDs was explored in this part. With the mixture ethanol/water (2:1) as solvent of $Pb(NO_3)_2$, the samples shown in Figure 5a-5c were formed with the concentration of $Pb(NO_3)_2$ 0.02 M (S3), 0.03 M(S4) and 0.04 M (S5). It is obvious that the size of PbS QDs increases significantly with the increasing concentration of $Pb(NO_3)_2$. This is in good accordance with thermodynamic theory, in which the driving force for crystal growth upon concentration

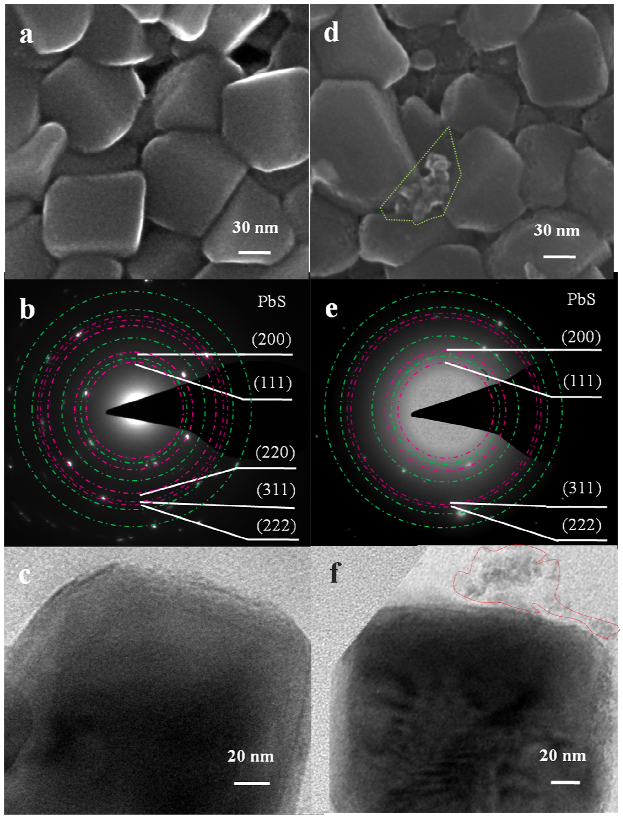

Figure 3 SEM and TEM images of PbS QDs-ZnO heterostructure formed in $Pb(NO_3)_2$ solutions with the volume ratio of ethanol/water: (a-c) 1:1; (d-f) 1:2.

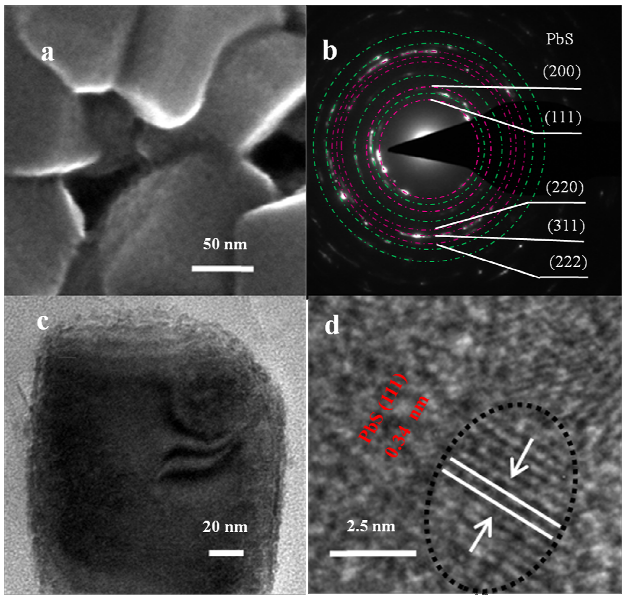

Figure 4 (a) SEM and (b)-(d) TEM images of PbS QDs-ZnO heterostructure formed in $Pb(NO_3)_2$ solutions with volume ratio of ethanol/water 2:1.

is estimated by the chemical potential tendency (μ). Generally, the chemical potential tendency (μ) can be described as the function of temperature (T) and variations in concentration ($\Delta c = c - c_0$) as shown in Equation 1:

$$\mu = \mu_0 + \gamma \times \Delta c \quad (1)$$

where μ_0 is the chemical potential for solution with the concentration c_0, γ is concentration coefficient, which is closely related with the solvent, concentration of ions, ions dispersion degree, and so on. With the concentration of $Pb(NO_3)_2$ increased, higher chemical potential is obtained which facilitates the absorption of Pb^{2+} onto the substrate, which will surely facilitate their reaction with S^{2-} and the crystal growth in the following SILAR circles. Large size QDs are thus obtained by increasing the concentration of $Pb(NO_3)_2$ within a suitable scale as shown in Figure 5c. Large size PbS nanoflakes were obtained when the concentration of $Pb(NO_3)_2$ increased to 0.04 M as illustrated in Figure 5c (EDS characterization of this sample is given in Supporting S3). This variation of PbS structure from nanodots to nanoflakes indicates that the formation of PbS by SIALR method is very sensitive to concentration variations and one should suit concentration to specific applications. This result can be commonly accepted, but there is one thing that is noteworthy to remind that the concentration coefficient γ is also in close relationship with the degree of saturation. As a result, one should adjust the concentration of ions with the solubility of the as-used solvent. This result is verified by sample in Figure 5d formed by using pure ethanol as solvent. The concentration of $Pb(NO_3)_2$ in ethanol was 0.0025 M, which is about ten times lower than the as-synthesized sample in Figure 5a. But larger size PbS QDs were also obtained in Figure 5d owing to the fact that the solubility of $Pb(NO_3)_2$ in ethanol at room temperature (about 0.025 M) is about 75 times lower than that in aqueous (1.8 M).

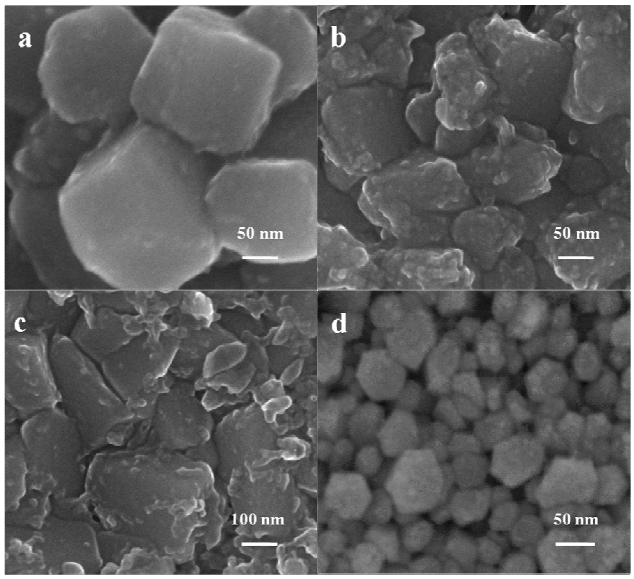

Figure 5 SEM images of PbS QDs-ZnO heterostructures formed by SILAR method with (a)-(c) ethanol/water mixture and (d) pure ethanol as solvents of $Pb(NO_3)_2$ solutions. The concentration of $Pb(NO_3)_2$ are (a) 0.02 M; (b) 0.03 M; (c) 0.04 M; (d) 0.0025M.

c. Effect of dipping times

Figure 6a-6c are SEM images of PbS QDs-ZnO heterostructure formed by dipping the samples into $Pb(NO_3)_2$ solutions for 1 time (S3), 3 times (S6) and 5 times (S7) in each circle. As shown in Figure 6b-6c, large size PbS blocks among ZnO nanorods are observed. Judging from the enlarged images shown the inset graphs in Figure 6a-6c, a rougher PbS layer is obtained on ZnO NCs for the samples with more dipping times in $Pb(NO_3)_2$ solutions. EDS results of S3, S6 and S7 are given in Figure 6d-6f. The stoichiometric ratio of Pb and S of the as-synthesized samples, which is theoretically calculated to be in close relationship with band gap modulation in Jeffrey C. Grossman's report,[18] is 4.25, 6.8 and 26.5, which confirms the effective regulation of Pb/S stoichiometric ratio by SILAR times. This exploration may thus provide another effective way for band gap modulation. One thing that is noteworthy to point out is that ZnO NRs is used instead of NC(s) due to their wide applications. Similar effect of dipping times on the PbS QDs formed on ZnO NC heterostructures is also observed as shown in supporting information S4.

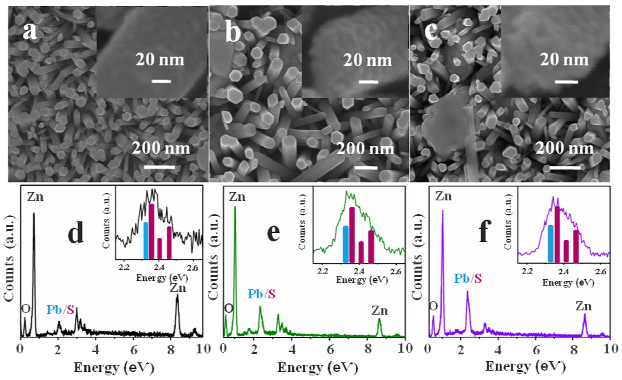

Figure 6 SEM images of PbS QDs-ZnO heterostructures formed by SILAR method with different dipping times in $Pb(NO_3)_2$ solution each circle: (a) 1 time; (b) 3 times; (c) 5 times and (d-e) Energy spectrum of S1, S6 and S7 and their insets are enlarged energy spectrum which shows peak positions of Pb and S elements by blue and peak columns.

Mechanism analysis on the formation of PbS QDs by SILAR method

Based on the above analysis, the formation of PbS QDs by SILAR method is illustrated in Figure 7. The schematic diagram (I)-(VI) in Figure 7 shows detail procedures for SILAR method mentioned in this article. Different from the common route, the sample was washed by pure ethanol and blew to dry, which may prompt more ions adsorption to the side surface of ZnO NCs. For SILAR procedures (I)-(II), Pb^{2+} cations are adsorbed onto ZnO surface, then, PbS is formed when the samples were dipped into Na_2S solution. Even all samples were dipped into the same Na_2S solution, PbS QDs with different structure and distribution are observed by using different $Pb(NO_3)_2$ solutions. Based on the theory in book Nano-Surface Chemistry on the formation of alcohol cluster adsorbed on the surfaces and the long-range attraction associated with such adsorption,[30] it is rational to predict that the distribution of PbS QDs is solvent-related. With ethanol/water volume ratio 1:2, these surfaces are strongly hydrophobic with corresponding advancing and receding large solution cluster contact angles as shown in Figure 7a. Consequently, the probability for Pb^{2+} adsorbed onto surface of ZnO was decreased and more PbS clusters are formed beyond the surface of ZnO. Increase in the proportion of ethanol in mixture

further decreases the liquid–vapor surface tension, giving a smaller solvent-surface attraction and contact angle of solution cluster on ZnO leading to a more equally distributed of Pb^{2+} ionic layer and eventually PbS QDs (Figure 7b-7c). Most interestingly, with the contact angle of Pb^{2+} growth cells, they can be spread more intensively at interfaces, which results in the formation of closely connected QDs in Figure 7c. Meanwhile, the size and morphology of the as-synthesized can be effectively tuned by concentration modulation. This process is believed to be thermodynamics dependence. Increase in the concentration always results in larger size PbS QDs due to the increasing chemical potential. Besides, stoichiometric ratio of Pb and S of PbS QDs can be controlled by dipping times through tuning the thickness of adsorbed layer of Pb^{2+} cations.

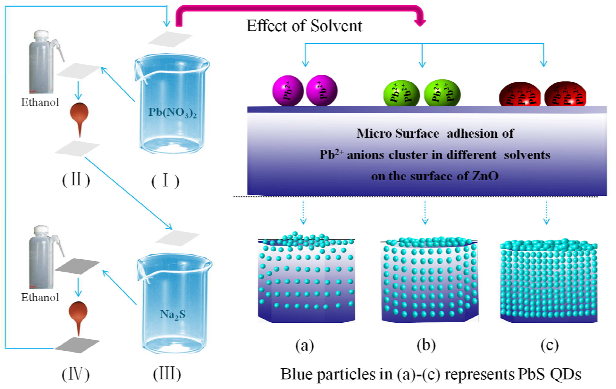

Figure 7 Schematic diagram of the procedures (I)-(IV) of SILAR method and formation of PbS QDs on ZnO with volume ratio of ethanol/water in $Pb(NO_3)_2$ solutions: (a) 1:2; (b) 1:1; (c) 2:1. The pink, green and red particles represent Pb^{2+} clusters and the blue particles present PbS QDs formed on ZnO in different solvents.

Characterization on optical and electrical properties

Due to the significant role of optical property to device applications, especially for solar cells and displays, the optical properties of the as-synthesized samples S1, S2 and S3 were explored in this part. High intensity light absorption peak at around 365 nm corresponding to the light absorption of ZnO is observed in each sample. Judging from Figure 8a, it is obvious that light absorption in both ultraviolet region and visible region is enlarged by decorating ZnO with PbS QDs. The absorption of sample S3, which is formed in $Pb(NO_3)_2$ solutions with the volume ratio of ethanol/water 2:1, increases the most. Generally, the band gap of QDs is size-dependent, which can be calculated as follows:[31]

$$E_{g,QD} = E_g + \frac{\hbar^2\pi^2}{2R^2}\left(\frac{1}{m_e^*} + \frac{1}{m_h^*}\right) \quad (2)$$

Where $E_{g,QD}$ is the bang gap of PbS QDs, E_g is the native band gap of PbS, R is the radius of PbS QDs, m_e^* and m_h^* are the effective mass of electrons and holes of PbS, $\hbar$ is Planck constant divided by π. The calculated size of PbS QDs corresponding to light absorption at 400 nm~1000 nm is 1.8 nm ~ 3.3 nm indicating the formation of small size PbS QDs. However, there are two thing that is noteworthy to point out: Firstly, the calculated size mentioned above may be smaller than the as-synthesized PbS QDs. Secondly, there is no obvious absorption peaks of PbS QDs existing in this spectrum. These can be explained as follows: (1) Wide size distribution of PbS QDs on ZnO surface and (2) The existence of elliptic QDs. (3) The effects coming from the interface between ZnO and PbS, on which more intensive experiments and analysis are still needed. Besides, the light absorption ratio of PbS QDs sensitized ZnO heterostructures in visible region and ultraviolet region is also solvent related as illustrated by the normalized absorption curves in Figure 8b. All these enlargements, which are of great significance for solar cell applications, can be attributed to the coverage of small size PbS QDs on the surface of ZnO. For the effect of coverage of PbS QDs on the optical band gap of ZnO, fine graph of ZnO bandgap-related absorption peaks at around 365 nm is given in the inset spectrum in Figure 8b. It is rational to believe that the optical bandgap characteristic of ZnO can also be tuned slightly by SILAR parameters, which is totally important to the band gap modulation of heterostructure and their device applications. More importantly, the solvent used for SILAR method also affect the electrical property of the as-synthesized heterostructure as shown in Figure 9. As it is well known that the I-V characteristics play key role for device performance, this exploration on solevnt-related electrical property is thus fundamental and necessary for their potential applications. ZnO NWs are firstly formed on quartz substrate by hydrothermal method. The I-V curve characterization mentioned here is performed by forming indium electrodes on ZnO NW arrays before SILAR and PbS/ZnO heterostructure after SILAR as shown in the inset of Figure 9. For pure ZnO, a liner I-V cure is observed as shown by black circle curve in Figure 9. With PbS formed on ZnO, obvious rectifying characteristics are obtained. The pink and blue circle curves belong to PbS QDs-on-ZnO heterostructure by using ethanol/water mixture (V/V=2:1) and pure water as solvent, respectively. Judging from the I-V result, the introduction of ethonal in the solvent of $Pb(NO_3)_2$ lead to a better rectifying performance with lower reverse current, which may significantly improve the performance of the as-synthesized optoelectronic devices.

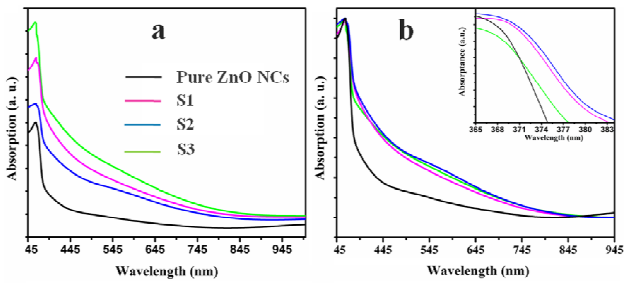

Figure 8 (a) Absorption spectrum S1, S2 and S3. Inset graph in Figure 7a is the enlarged absorption spectrum of ZnO absorption peaks in Figure 7b.

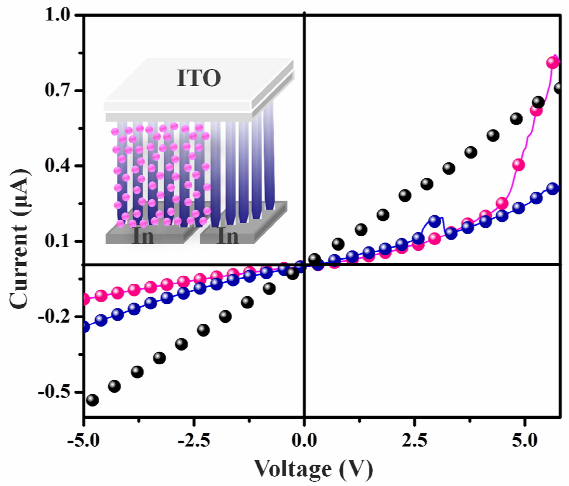

Figure 9 I-V curve of ZnO/PbS heterostructures formed in $Pb(NO_3)_2$ solution with different solvents. The inset is the skematic diagram of the fabricated device.

Conclusion

Small size PbS QDs (<5 nm) are formed on the surface of ZnO by room temperature successive ionic layer adsorption and reaction method. Controllable growth of PbS QDs-ZnO heterostructures is achieved by adjustments of growth parameters including solvent and concentration of $Pb(NO_3)_2$ solutions as well as SILAR times. The distribution of PbS QDs on ZnO is mainly solvent related and well-distributed PbS QDs is achieved with the volume ratio of ethanol/water in $Pb(NO_3)_2$ solution larger than 1:1. Exploration on the relationship between the structure as well as the stoichiometric ratio of PbS QDs and the growth parameters including concentration and SILAR times indicates that tunable growth of PbS QDs is feasible. The beginning of PbS growth on ZnO is discussed from the points of solvent-related-variations in interaction between the growth cells and interface surface and continued with thermodynamic-domained crystal growth process. In order to further improve the potential technique applications and device performance of theses PbS QDs-ZnO heterostructures, effect of solvent on the optical and electrical properties of the as-synthesized heterostructures are also explored, which shows a substantially increase in the light absorption in the visible range and improvement in their rectifying performance.

ACKNOWLEDGMENTS

This work is supported by National Science Foundation (No. 61306014); Open Project Program of Key Laboratory for Photonic and Electric Bandgap Materials, Ministry of Education, Harbin Normal University (No. PEBM201302).

Notes and references

[a] *School of Materials Science and Engineering, Harbin Institute of Technology, Harbin 150001, P. R. China; E-mail: shujijiao@gmail.com*
[b] *Key Laboratory for Photonic and Electric Bandgap Materials, Ministry of Education, Harbin Normal University, Harbin, 150025, P. R. China*

References:

1 C-H. M. Chuang, P. R. Brown, V. Bulović, M. G. Bawendi, *Nat. Mater.,* 2014, **13**,796.
2 P. V. Kamat, *J. Phys. Chem. Lett.*, 2013, **4**, 908–918.
3 M-J Choi, J Oh, J-K. Yoo, J. Choi, D. M. Sim and Y. S. Jung, *Energ. Environ. Sci.*, 2014, **7**, 3052.
4 M. Heiss, Y. Fontana, A. Gustafsson, G. Wüst, C. Magen, D. D. O'Regan, J. W. Luo, B. Ketterer, S. Conesa-Boj, A. V. Kuhlmann, J. Houel, E. Russo-Averchi, J. R. Morante, M. Cantoni, N. Marzari, J. Arbiol, A. Zunger, R. J. Warburton and A. F. i Morral, *Nat. Mater.,*2013,**12**,439.
5 A. G. Pattantyus-Abraham, I. J. Kramer, A. R. Barkhouse, X. Wang, G. Konstantatos, R. Debnath, L. Levina, I. Raabe, M. K. Nazeeruddin, M. Gra¨tzel, and E. H. Sargent, , Acs nano, 2010,**4**,3374.
6 L. Cademartiri, E. Montanari, G. Calestani, A. Migliori, A. Guagliardi and G. A. Ozin, *J. Am. Chem. Soc.,* 2006, **128**, 10337.
7 R. J. Ellingson, M. C. Beard, J. C. Johnson, P. Yu, O. I. Micic, A. J. Nozik, A. Shabaev and A. L. Efros, *Nano Lett.*, 2005, **5**, 5865.
8 D Wang, J Qian, F Cai, S He, S Han and Y Mu, *Nanotechnology,*2012, **23**, 245701.
9 S. A. McDonald1, G. Konstantatos1, S. Zhang, P. W. Cyr, E. J. D. Klem1, L. Levina1 and E. H. Sargent1, *Nat. Mater.,*2005, **4**, 138.
10 I. Moreels, Y. Justo, B. D. Geyter, K. Haustraete, J. C. Martins and Zeger Hens, *ACS Nano*, 2011, **5**, 2004.
11 I. Moreels, K. Lambert, D. Smeets, D. D.Muynck, T. Nollet, J. C. Martins, F. Vanhaecke, A. Vantomme, C. Delerue, G. Allan and Z. Hens, *ACS Nano*, 2009, **3**, 3023.
12 L. Tao, Y. Xiong, H. Liu and T. Shen, *Nanoscale,* 2014, **6**, 931.
13 Q. Kang, S. Liu, L. Yang, Q. Cai and C. A. Grimes, *App. mater. inter.*,2011,**3**,746;
14 H. J. Lee, J. Bang, J. Park, S. Kim and S-M Park, *Chem. Mater.*,2010,**22**, 5636
15 V. González-Pedro, C. Sima, G. Marzari, P. P. Boix, S. Giménez, Q. Shen, T. Dittrich and I. Mora-Seró, *Phys. Chem. Chem. Phys.*, 2013,**15**, 13835.
16 Y. Li**,** L. Wei**,** X. Chen**,** R. Zhang**,** X. Sui**,** Y. Chen**,** J. Jiao and L. Mei**,** *Nanoscale Res. Lett.,* 2013, **8**,67 ; N. Zhou, G. Chen, X. Zhang, L. Cheng, Y. Luo, D. Li and Q. Meng, *Electrochem. Commun.*, 2012, **20**, 97.
17 J. Puišo , S. Lindroos, S. Tamulevičiusa, c, M. Leskeläb and V. Snitka, *Thin Solid Films*, 2003, **428**, 223.
18 D. Kim, D-H Kim, J-H Lee and J. C. Grossman, *Phys. Rev. Lett.*, 2013, **110**,196802.
19 J. Jean, S. Chang, P. R. Brown, J. J. Cheng, P. H. Rekemeyer, M. G. Bawendi, S. Gradečak and V. Bulović1, *Adv. Mater.*, **2013**, *25*, Issue 20, 2790.
20 H. L. Li, S. J. Jiao, S. S. Bai, H. T. Li, S. Y. Gao, J. Z. Wang, Q. J. Yu, F. Y. Guo and L. C. Zhao, *Phys, Status. Solidi. A*, 2014, **211**,595.
21 H. L. Li, S. J. Jiao, S. Y. Gao, H. T. Li and L. Li, *Cyst. Eng. Comm.*, 2014, **16**, 9069.
22 R. G. Pérez, G. H. Téllez, U. P. Rosas, A. M. Torres, J. H. Tecorralco, L. C. Lima and O. P. Moreno, *J. Mater. Sci. and Engineer.*, 2013, **A 3**, 1.
23 J. Lee, J. Bang, J. Park, S. Kim and S-M Park, *chem. Mater.* 2010,22, 5363.
24 J. Yang, T. Ling, W-T Wu, H Liu, M-R Gao, C. Ling, L. Li and X-W Du, *Nat. Commun.,* 2013, **4**, 1695.
25 O. M. Ntwaeaborwa, R. E. Kroon, V. Kumar, T. Dubroca, J-P Ahn, J-K Park, H. C. Swart, *J. Phys. Chem. Solids*, 2009, **70**, 1438.
26 Y. V. Yermolayeva, Y. N. Savin, A. V. tolmachev, *Solid State Phenomena,* 2009 **151**, *264.*
27 A. Chahadih**,** H. E. Hamzaoui**,** R. Bernard**,** L. Boussekey**,** L. Bois**,** O. Cristini**,** M. L. Parquier**,** B. Capoen and M. Bouazaoui' *Nanoscale Res. Lett.,* 2011, **6**, 542.
28 E. Kokkoli and C. F. Zukoski, *J. Colloid &Interf. Sci.*, 1999, **209**, 60.
29 D. Y. C.Chan, D. J. Mitchell, B. W. Ninham and B. A. Pailthorpe, *Mol. Phys.*, 1978, **35**, 1669.
30 Morton Rosoff, in *Nano-Surface Science*, ed. Marcel Dekker, Inc, Madison Avenue, 2002, Ch. 1, pp. 13.
31 Y. Wang, A. Suna, W. Mahler and R. Kasowski, *J. Chem. Phys.*, 1987, **87**, 7315; A. Sashchiuk, E. Lifshitz, *J. Sol-Gel Sci. Techn.*, 2002, **24**, 31.

Graphical abstract

Manuscript ID CE-ART-02-2015-000292

Title: Tunable Growth of PbS Quantum Dots-ZnO Heterostructure and Mechanism Analysis

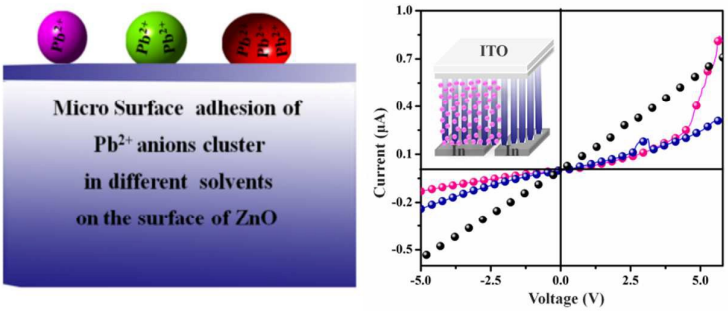

Tunable growth of PbS-QDs-on-ZnO heterostructure by SILAR method and mechanism analysis at microscope.